

ORIGINAL ARTICLE

Iran J Allergy Asthma Immunol

April 2022; 21(2):151-166.

Doi: 10.18502/ijaai.v21i2.9223

Agent-based Modeling of Tumor and Immune System Interactions in Combinational Therapy with Low-dose 5-fluorouracil and Dendritic Cell Vaccine in Melanoma B16F10

Sarah Rahbar¹, Sajad Shafiekhani¹, Armin Allahverdy², Arezoo Jamali^{3,4}, Nasim Kheshtchin^{5,6}, Maryam Ajami⁷, Zahra Mirsanei⁸, Sima Habibi⁹, Bahador Makkiabadi^{1,10}, Jamshid Hadjati⁹, and Amir Homayoun Jafari^{1,10}

¹ Department of Medical Physics and Biomedical Engineering, School of Medicine, Tehran University of Medical Sciences, Tehran, Iran

² Department of Radiology, Sari School of Allied Medical Sciences, Mazandaran University of Medical Sciences, Sari, Iran

³ Department of Molecular Medicine, Faculty of Advanced Technologies in Medicine, Iran University of Medical Sciences, Tehran, Iran

⁴ Molecular Biotechnology and Gene Therapy, Paul-Ehrlich-Institut, Langen, Germany

⁵ Allergy Research Center, Shiraz University of Medical Sciences, Shiraz, Iran

⁶ Department of Immunology, School of Medicine, Shiraz University of Medical Sciences, Shiraz, Iran

⁷ Department of Immunology, Faculty of Medical Sciences, Tarbiat Modares University, Tehran, Iran

⁸ Department of Immunology, School of Medicine, Shahid Beheshti University of Medical Sciences, Tehran, Iran

⁹ Department of Immunology, School of Medicine, Tehran University of Medical Sciences, Tehran, Iran

¹⁰ Research Center for Biomedical Technologies and Robotics (RCBTR), Tehran University of Medical Sciences, Tehran, Iran

Received: 30 September 2021; Received in revised form: 7 October 2021; Accepted: 13 October 2021

ABSTRACT

This study is designed to present an agent-based model (ABM) to simulate the interactions between tumor cells and the immune system in the melanoma model. The Myeloid-derived Suppressor Cells (MDSCs) and dendritic cells (DCs) are considered in this model as immunosuppressive and antigen-presenting agents respectively.

The animal experiment was performed on 68 B16F10 melanoma tumor-bearing C57BL/6 female mice to collect dynamic data for ABM implementation and validation. Animals were divided into 4 groups; group 1 was control (no treatment) while groups 2 and 3 were treated with DC vaccine and low-dose 5-fluorouracil (5-FU) respectively and group 4 was treated with both DC Vaccine and low-dose of 5-FU. The tumor growth rate, number of MDSC, and presence of CD8+/CD107a+ T cells in the tumor microenvironment were evaluated in each group. Firstly, the tumor cells, the effector immune cells, DCs, and the MDSCs have been considered as the agents of the ABM model and their interaction methods have been extracted from the literature

Corresponding Author: Amir Homayoun Jafari, PhD;
Department of Medical Physics and Biomedical Engineering, School
of Medicine, Tehran University of Medical Sciences, Tehran, Iran.

Tel: (+98 21) 6405 3252, Fax: (+98 21) 6405 3242,
E-mail: h_jafari@sina.tums.ac.ir

and implemented in the model. Then, the model parameters were estimated by the dynamic data collected from animal experiments.

To validate the ABM model, the simulation results were compared with the real data. The results show that the dynamics of the model agents can mimic the relations among considered immune system components to an emergent outcome compatible with real data. The simplicity of the proposed model can help to understand the results of the combinational therapy and make this model a useful tool for studying different scenarios and assessing the combinational results.

Determining the role of each component helps to find critical times during tumor progression and change the tumor and immune system balance in favor of the immune system.

Keywords: Fluorouracil; Melanoma; Myeloid-derived suppressor cells; Tumor microenvironment

INTRODUCTION

The presence of myeloid-derived suppressor cells (MDSCs) in the tumor environment was detected in cancer patients about 30 years ago.¹⁻⁴ However, their functions have recently drawn the attention of scholars in the field. Since the accumulation of these cells in the tumor environment can suppress the immune response to disease or cancer, they may play a significant role in the progression and metastasis of various cancers.^{5,6} One of the most important characteristics of MDSCs is the suppression of T cell responses and their specific immunosuppression. There are several strategies for removing MDSCs in the tumor environment.⁷ It has been shown that the prescription of low doses of 5-Fluorouracil (5-FU) that is a cytotoxic chemotherapy medication used to treat multiple solid tumors, can result in stability in MDSC removal and greatly reduce the problem of the regrowth of MDSCs.⁸

Antigen-presenting cells, especially dendritic cells (DC), have a crucial role in inducing an antitumor immune response and controlling tumor growth. However, there is a delay between the detection of tumor antigens by the antigen-presenting cells (APCs) and the adaptive immune responses to become established. This time delay can give the tumor a chance to grow and escape the immune system which causes tumor progression. DC vaccination is an active immunization approach that can boost the adaptive immune response and enhance it. Therefore, it is considered a promising method for the treatment of cancers.

Understanding relations among immune system components and their interactions result in better cancer treatments. New immunotherapy methods are

based on the new finding in tumor and immune system interactions and the effect of the drugs and interventions. Because In vivo application of multiple methods of treatment is expensive and time-consuming; using mathematical models as a tool to test and predict the results of different hypothesis are useful. So far, many mathematical models have been proposed to examine the interactions between the immune system and the tumor. Many of these models are based on ordinary differential equations (ODEs). The first mathematical models have mainly studied the growth of tumor cells without the presence of the immune system.^{9,10} In these models, tumor growth was merely considered as a differential equation. In subsequent studies, other factors such as cytotoxic T-lymphocytes, interleukin (IL)-2 cytokines, tumor growth factor-beta (TGF- β), and other factors were added to the models, respectively.¹¹⁻¹⁴ Other methods of modeling such as agent-based modeling (ABM) have been proposed to investigate the interactions between the immune system and tumor cells.¹⁵⁻¹⁷ Specific advantages of agent-based models include their ability to model individual functioning entities and their interactions, to incorporate a global process, and achieve an emergent result. The agents are dynamically linked in such a way that they can form very complex structures and feedback networks with simple rules and actions. This simplicity in presentation and form makes ABM a good choice for modeling complex dynamical systems of multiple agents with intertwined relations. So far, modeling the interactions between the immune system and tumor cells in the presence of MDSCs and the effect of its elimination has been less focused on by researchers who are working in this field. It is also

Low-dose 5-Fluorouracil and Dendritic Cell Vaccine Combination Therapy

important to notice that the immune system has several mechanisms to balance and control the immune response by activating immunosuppressive agents and cytokines.

Therefore, in this study, an ABM model was first proposed to examine the interactions between the immune system and tumor cells with the presence of MDSCs. Then, the effects of the low-dose 5-FU on MDSC removal and DC vaccine are added to this model. To access actual laboratory data, an animal model is introduced. To optimize the initial structure of the model, based on the data obtained from the control group of the animal model in which no intervention was performed, the parameters of the model are estimated; using the genetic algorithm (GA). The tumor volume, MDSCs percentage, and the number of effective immune cells obtained from model simulation are presented as the results of the ABM model. The obtained results are interpreted once, regardless of the injection of the low-dose 5-FU drug and DC vaccine, and again after implementing the effects of low-dose 5-FU and vaccine. The model is validated by comparing the results with the experimental data from the combinational therapy group of the animal model.

MATERIALS AND METHODS

Animals and Cell Line

Seventy-five mice (6 to 8 weeks old C57BL/6 Female) were purchased from the Pasteur Institute of Iran and kept in the animal lab of the Department of Immunology, School of Medicine, TUMS. Sixty-eight of them were divided into 4 groups and the rest were used for DC culture. C57BL/6 derived melanoma (F10-B16: ATCC CCL-6475TM) cell line (available in Department of Immunology) were cultured in in-vitro culture in Roswell Park Memorial Institute Medium (RPMI 1640) (Biosera, Korea) which was supplemented with 10% heat-inactivated fetal bovine serum (Gibco, Grand Island, NY, USA), 2 mL glutamine (Sigma, USA), 100 µg/mL streptomycin, and 100 U/mL penicillin. All procedures on animals were performed according to the ethical committee protocols published by TUMS (1394.474).

DC Preparation and Culture

Generation of Bone Marrow-Derived DCs (BMDCs) was performed mainly based on Inaba protocol.¹⁸ Cells were harvested from the femurs and

tibias of the C57/BL6 mice. Then red blood cells were removed, and the rest (5×10⁵ cells/mL) were cultured in RPMI 1640b (Gibco, USA) medium supplemented with 10% heat-inactivated fetal bovine serum (Gibco, USA), 20 ng/mL of recombinant murine GM-CSF (PeproTech, London, UK), and 10 ng/mL of recombinant murine IL-4 (PeproTech, London, UK), 2mM L-glutamine (Biosera, UK), 100 µg/mL streptomycin, and 100 U/mL penicillin. The culture medium was replaced with fresh media on days 3 and 5. Immature DCs were pulsed on day 6 with 100 µg/mL tumor cell lysate (for 18 h) prepared by subjecting 4 × 10⁷ F10-B16 cells/mL in PBS to 6 cycles of rapid freezing in liquid nitrogen and thawing at 37°C. The lysates were spun at 900 g for 10 min to remove particulate cellular debris. The resulting supernatants were filtered by 0.2 µm membrane and stored. Dendritic cells were then stimulated by adding 10 µg CpG 1826, and 6 µg *Listeria monocytogenes* lysate (LML) 14 h before harvesting cells on day 5.¹⁹ On day 7, non-adherent mature (m) DCs were harvested. The morphology of mDCs was assessed by cytospin preparation of the cells; using Giemsa stain.

RNA Isolation and Real-time Quantitative PCR

RNA was extracted from frozen tumor and spleen tissues by using a Hybrid-R RNA purification kit (GeneAll Biotechnology, Korea). One microgram of RNA was reverse transcribed into complementary DNA (cDNA); using QuantiTect Reverse Transcription kit (Qiagen, Germany). cDNAs were quantified by real-time PCR; using an SYBR Green real-time PCR master mix (Primer design, UK) on an ABI 7500 detection system (Applied biosystems). Relative mRNA levels were assigned; using the ΔCt method. Values were expressed relative to housekeeping genes such as *β-actin*. Supplementary Table S1 lists the primers used in real-time PCR tests.

Flow Cytometry

Single-cell suspensions were stained; using the following fluorescently labeled antibodies: APC-conjugated anti-CD3, anti-CD107a, and anti-Gr-1 or FITC-conjugated anti-CD8 or PE-conjugated anti-CD11b; or matched, fluorochrome-labeled isotype control monoclonal antibody (all purchased from Biolegend, USA). Flow cytometry was conducted; using a FACSCalibur flow cytometer (Becton-

Dickenson, Mountain View, CA, USA) and analyzed with FlowJo software.

In vivo Antitumor Experiments

Mice were divided into the following 4 groups (n=17 mice each): 1) Control (PBS control), 2) low-dose 5-FU therapy, 3) DC vaccine therapy and 4) combinational therapy of low-dose 5-FU and DC vaccine. On the day0 of the experiment, all mice were subcutaneously injected by B16/F10 tumor cells (5×10⁶ cells) in the right flank. For low-dose 5-FU and combinational therapy groups, mice were injected intraperitoneally with 5-FU (50 mg/kg) every 3 days, starting from day 0 to day 24. Mice in other groups received PBS instead of low-dose 5-FU on the same days. For the DC vaccine and combinational therapy groups, a single dose of DC vaccine (10⁶) is applied on day 0 around tumor sites. Tumor sizes in all groups were assessed by measuring the shortest (A) and longest (B) diameters of the tumors by digital caliper on days 11, 12, 14, 15, 17, 18, 19, 22, and 24. These diameters were used to estimate tumor volume by elliptical volume equation ($V = \frac{4}{3} \pi AB^2$). For Flow cytometry assay and Real-time-PCR, on days 13, 17, 19, 22, and 25, two or three mice were collected randomly and sacrificed.

The Agent-based Model

The model presented in this study is an ABM model of interactions between the immune system and tumor cells, in which MDSC suppressive effects are also considered. The model uses 8 biological variables including 4 cell types -Tumor, effector CD8+ cells, dendritic cells, and MDSCs - and 4 cytokines - TGF-β, IL-2, IL-10, and IFN-γ - which have pro-inflammatory and anti-inflammatory effects. It is assumed that the population of the tumor cells is homogenous and all the interactions within the cell groups are synchronized within a 24-hour duration. Therefore, all cells behave in the same way. This assumption is considered valid for other cell groups in the model.

Tumor cells are included and are denoted by the variable T (n), where n is the time in days. The logistic growth rate is applied to model the growth rate of the tumor when no therapy is applied. Also, NK and CD8+ T effector cells which are denoted by E(n) in the model are considered tumor-specific and can kill tumor cells. The model describes the dynamics of the interactions between these cells and the correlations between DC

and MDSCs with other agents. Cell populations and cytokines are considered as follows:

- $T(n)$, tumor population
- $E(n)$, effector cells population
- $DC(n)$, dendritic cell population
- $MDSC(n)$, MDSCs population
- $TGF-B(t)$, TGF-B-β concentration
- $IL10(n)$, IL-10 concentration
- $IL2(n)$, IL-2 concentration
- $IFN(n)$, IFN-γ concentration

The interactions between these agents are presented in Figure 1.

Model Equations

The implementation of the tumor and immune system model includes a set of differential equations. Our model has four various cells and four cytokines in the tumor microenvironment. Each equation represents the change in the number of cells or concentration of cytokines over time.

$$T(n + 1) = T(n) + \frac{a_1}{1 + b_1 \cdot TGF(n)} \cdot T(n) \left(1 - \frac{c_1}{d_1 + TGF(n)} \cdot T(n) \right) - P_{encounter} \cdot T(n) \cdot E(n) \tag{1}$$

$$P_{encounter} = \frac{e_1 \cdot IFN}{f_1 + IFN} + \frac{g_1}{1 + h_1 \cdot TGF} + \frac{k_1}{m_1 + MDSC} \tag{2}$$

In the first equation, the second term represents the logistic tumor growth that is affected by TGF-β concentrations. High concentrations of TGF-β can limit tumor growth, while low concentrations promote tumor growth. The last term in the first equation denotes effector cells killing tumor cells.

The second equation models the affinity of effector cells in the encounter with the tumor. This affinity is enhanced by IFN-γ which is a proinflammatory cytokine and reduced by TGF-β concentration and MDSC presence in the microenvironment.

$$E(n + 1) = E(n) + P_{recruitment} \cdot \frac{E(n)}{a_2 + E(n)} - R_E \cdot MDSC(n) \cdot E(n) - \mu_E \cdot E(n) \tag{3}$$

$$P_{recruitment} = \frac{b_2 \cdot DC(n)}{c_2 + DC(n)} + \frac{d_2 \cdot IL2(n)}{e_2 + IL2(n)} + \frac{f_2}{g_2 + IL10(n)} \tag{4}$$

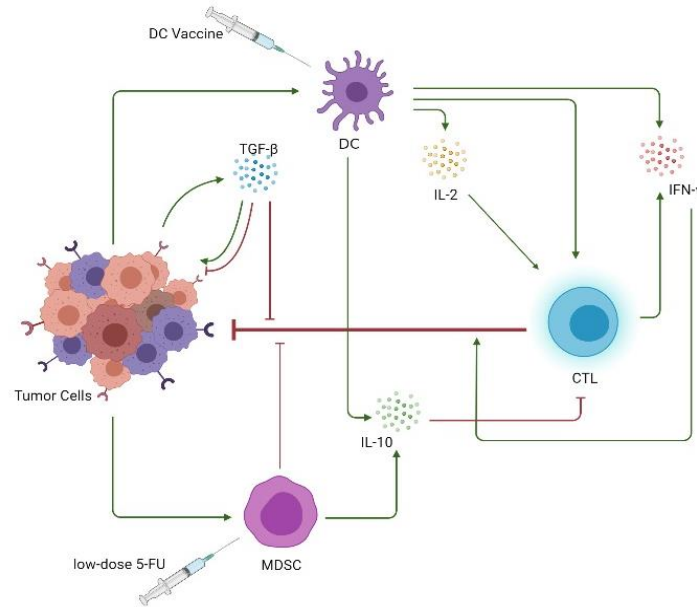


Figure 1. Interactions between agents of the model. Cell populations and cytokines are considered as agents that have interactions. The immune system components that are considered in the agent-based model (ABM) are presented in the diagram. The green arrows and red lines show the increasing effects and the inhibiting effects respectively. Figure created with BioRender.com.

Equations (3) and (4) model the effector cells' population. The second term in equation (3) represents proliferation and recruitment of effector cells to the tumor microenvironment due to the antigen-presenting of DC and IL-2 secretion. This function is also affected by the anti-inflammatory role of IL-10. The last term in equation (3) shows the half-life of the effector cells.

$$DC(n+1) = DC(n) + \frac{a_3 \cdot T(n)}{b_3 \cdot T(n)} - \mu_3 \cdot DC(n) \quad (5)$$

Antigen-presenting DCs are activated and proliferated in the presence of the tumor. This feature is modeled in the second term of equation (5). The negative term in the equation represents the cell death of DCs.

$$MDSC(n+1) = MDSC(n) + a_4 + \frac{b_4 \cdot T(n)}{c_4 + T(n)} - \mu_4 \cdot MDSC(n) \quad (6)$$

The second term in the above equation is the constant production rate of the MDSCs in the body and the third term represents the production and recruitment of MDSCs because of tumor growth. The last term models death of MDSCs.

$$TGF(n+1) = TGF(n) + \frac{a_5 \cdot T(n)^2}{b_5 + T(n)^2} - \mu_5 \cdot TGF(n) \quad (7)$$

Equation (7) determines the production of TGF-B by tumor cells and its decay over time.

$$IL2(n+1) = IL2(n) + \frac{a_6 \cdot DC(n)}{b_6 + DC(n)} - \mu_6 \cdot IL2(n) \quad (8)$$

IL-2 is mostly produced by antigen-presenting cells to enhance the affinity of adaptive immunity cells. Equation (8) assumes that DCs are the main source of IL-2 production and its decay during the time.

$$IL10(n+1) = IL10(n) + \frac{a_7 \cdot MDSC(n)}{b_7 + MDSC(n)} + \frac{c_7 \cdot DC(n)}{d_7 + DC(n)} - \mu_7 \cdot IL10(n) \quad (9)$$

IL-10 is assumed to be produced by MDSCs which are a part of the anti-inflammatory mechanism of adaptive immunity. This property is modeled in the second term of the equation (9). Also, DCs may produce IL-10 to balance the inflammation and play the role of a break in the intense response of the effector cells.

$$IFN(n+1) = IFN(n) + \frac{a_8 \cdot E(n)}{b_8 + E(n)} + \frac{c_8 \cdot DC(n)}{d_8 + DC(n)} - \mu_8 \cdot IFN(n) \quad (10)$$

Similarly, IFN-γ is an inflammatory agent and is produced by effector cells and antigen-presenting cells. IFN-γ is cleared from the microenvironment as well.

Low-dose 5-Fu Implementation

In several studies, the effect of 5-FU on the elimination of MDSCs is investigated. Vincent et al. assessed this effect in melanoma-bearing mice and Abedi-Valugherdi et al, have administered different doses to inspect their effect on different immune factors such as MDSC percentage in tumor and spleen.^{4,20} Shariatpanahi et al, have used these data in an ODE model to simulate 5-FU injection for tumor growth reduction.²⁵ Figure 2 shows the elimination of splenic MDSCs by using a single dose of 5-FU.

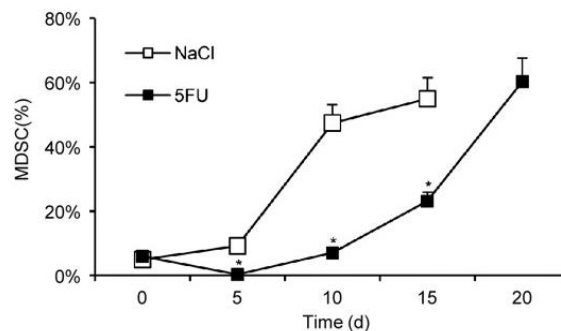


Figure 2. 5-Fluorouracil (5FU) eliminates myeloid-derived suppressor cells (MDSC) *in vivo*. Tumor-bearing mice were treated with low-dose 5FU and NaCl as a placebo. Spleens were harvested at various post-treatment times. The graphic shows the percentage of splenic MDSC in both groups.²⁰

According to the pharmacodynamics of 5-FU, and since the maximum effect of low-dose 5-FU occurs after the third day of injection, we injected multiple doses with 3 days intervals to maintain the effective concentration of the drug in our 5-FU treatment groups during the experiment.²⁰ To implement the effect of multiple doses of 5-FU injections in the model, we have extracted the differential sequence of MDSC values over time between the 5-FU treated and the placebo groups. Since these results are valid for a single dose, it is assumed that the effect of multiple doses can be represented by the superimposition of the reduction sequence on 5-FU injection times in the 5-FU therapy group (days 0 to 24, every 3 days). The resulting sequence was then applied with a tuning factor in saturation mode to b_2 coefficient of Equation (4) and with a scaled negative factor in MDSCs maturation and proliferation in equation (6).

The tuning factors are determined by validating the tumor and effector behavior in the 5-FU therapy group; using GA. Figure 3 represents the overall shape of the

Following the first goal of this study, the MDSCs were considered as a new agent in the ABM model and the role of these cells in suppressing the immune system response in interaction with tumor cells was introduced in the form of a new rule in the proposed model. To achieve the second goal of this study, the effect of a low-dose 5-FU drug was considered as an interventionist agent. As a result, the low-dose 5FU eliminates MDSCs. To develop a mathematical model of the low-dose 5-FU, firstly, its effect on MDSCs was investigated.

resulting single-dose and multiple-dose sequences.

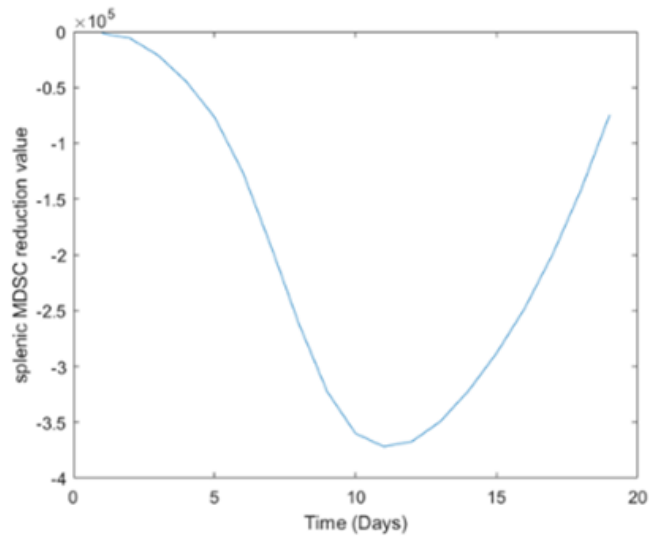
DC Vaccine Implementation

DC vaccine function is applied to the model by changing the initial condition of the model for the control group. For the DC vaccine therapy group, equation (5) is calculated with initial DC numbers 100 times more than the control group. This assumption is based on the DC population in C57BL/6 mice reported by Lee et al.²¹ Additionally, the combinational effect of the activated DC vaccine on the affinity of the effector cells is imposed by adding a saturating term to the equation (2).

Estimation of ABM Model Parameters

To optimize the initial structure of the ABM model, firstly, the parameters of the ABM model were estimated; using GA based on the data obtained from the control group of empirical data. Estimated values for the parameters; using the GA are shown in Table 1.

(a)



(b)

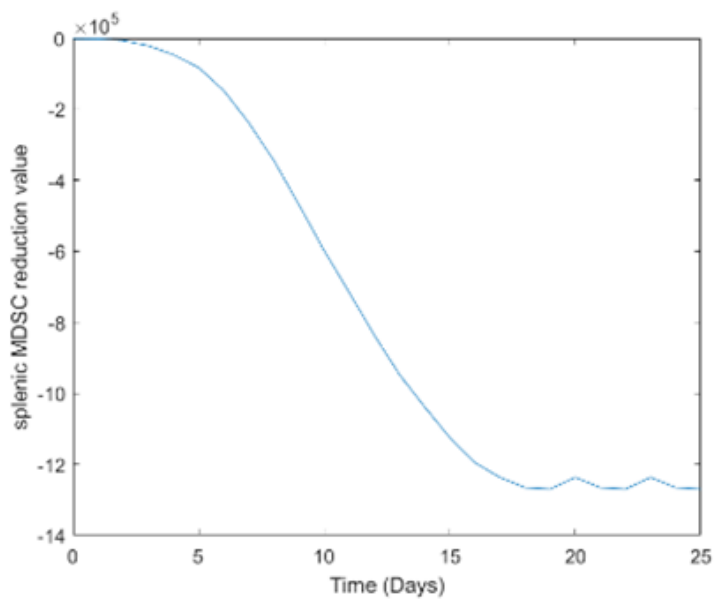


Figure 3. 5-Fluorouracil (5-FU) injection effect implementation in the model. (a) Overall shape of the reduction of splenic myeloid-derived suppressor cells (MDSCs) sequences for single low-dose 5-FU injection on day 0 and (b) for multiple-dose injections on days 0 to 24 every 3 days.

Table 1. Estimated parameters of the agent-based model (ABM) by genetic algorithm (GA). The fitness function is the mean squared error between model outputs and empirical data points in the control group.

Agent	Parameter	Description	value estimated
Tumor	a ₁	Maximum rate of Tumor growth coefficient	6.5
	b ₁	Half saturation rate of TGF-β on Tumor growth	31.7
	c ₁	Carrying capacity of Tumor growth	0.0001
	d ₁	Half saturation rate of TGF- β on maximum tumor size	6
	e ₁	The maximum rate of IFN-γ on effector affinity	0.0001
	f ₁	Half saturation rate of IFN-γ on effector affinity	134
	g ₁	The maximum rate of TGF- β on effector affinity	0.001
	h ₁	Half saturation rate of TGF-β on effector affinity	63
	k ₁	The maximum rate of MDSC on effector affinity	0.0003
	m ₁	Half saturation rate of MDSC on effector affinity	4.78
	Effector cells	a ₂	Half saturation rate of the effector proliferation and recruitment
R _E		Regulatory effect of the MDSCs on Effector cells	0.008
b ₂		The maximum rate of the DCs effect on effector proliferation and recruitment	2
c ₂		Half saturation rate of the DCs effect on effector proliferation and recruitment	4.24
d ₂		Maximum rate of the IL-2 effect on effector proliferation and recruitment	0.001
e ₂		Half saturation rate of the IL-2 effect on effector proliferation and recruitment	0.18
f ₂		Maximum rate of the IL-10 effect on effector proliferation and recruitment	1.62
g ₂		Half saturation rate of the IL-10 effect on effector proliferation and recruitment	9
	μ _E	death rate of effector cells	0.09
DC	a ₃	Maximum rate of the Tumor effect on DCs proliferation	2.43*10 ⁴ (27)
	b ₃	Half saturation rate of the Tumor effect on DCs proliferation	100 (27)
	μ ₃	the death rate of DCs	0.231 (27)
MDSC	a ₄	minimum production rate of MDSCs	0.018
	b ₄	The maximum rate of the Tumor effect on MDSC proliferation	0.4
	c ₁	Half saturation rate of the Tumor effect on MDSC proliferation	50
	μ ₄	the death rate of MDSCs	0.2423
TGF-β	a ₅	The maximum rate of the Tumor effect on TGF-β production	7.177
	b ₅	Half saturation rate of the Tumor effect on TGF-β production	0.3919
	μ ₅	TGF-B half-life rate	0.55
IL-2	a ₆	The maximum rate of the DCs effect on IL-2 production	0.067
	b ₆	Half saturation rate of the DCs effect on IL-2 production	28
	μ ₆	IL-2 half-life rate	0.007
IL-10	a ₇	Maximum rate of the MDSCs effect on IL-10 production	0.02
	b ₇	Half saturation rate of the MDSCs effect on IL-10 production	257
	c ₇	Maximum rate of the DCs effect on IL-10 production	0.21
	d ₇	Half saturation rate of the DCs effect on IL-10 production	17.3
	μ ₇	IL-10 half-life rate	0.01
IFN- γ	a ₈	Maximum rate of the effectors effect on IFN- γ production	1.9
	b ₈	Half saturation rate of the effectors' effect on IFN- γ production	60
	c ₈	The maximum rate of the DCs effect on IFN- γ production	0. 1
	d ₈	Half saturation rate of the DCs effect on IFN- γ production	212.2
	μ ₈	IFN- γ half-life rate	0.009

Low-dose 5-Fluorouracil and Dendritic Cell Vaccine Combination Therapy

ABM Model Simulation

In the first step, according to the agents considered for the ABM model and based on the interactions between these agents that were introduced in equations (1-10), and using the parameters applied for the ABM model in the absence of treatment. The ABM model was simulated by MATLAB software (the MathWorks Company, Inc.). In this step, the size of the tumor, the number of effector cells, and the percentage of MDSCs obtained from the simulation of the ABM model were recorded from days 13 to 25.

In the second step, the effect of 5-FU injections and the DC vaccine was also applied in the model. For this purpose, 5-FU and DC vaccine effects were considered as the input of the ABM model. The interactions between the model's agents were calculated based on

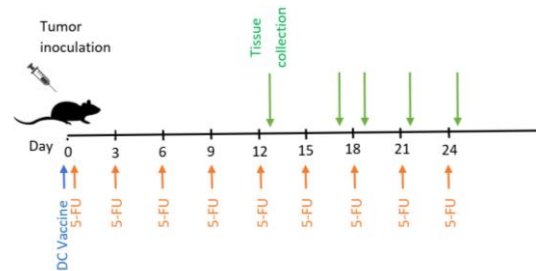
equations (1-10) and 5-FU and DC vaccine implementations discussed earlier. The tumor growth rate and overall dynamics of the agents in therapy groups are considered model outputs.

RESULT

The Results of Animal Experiment

As mentioned earlier, the designed animal model was consisting of 4 groups of C57BL/6 tumor-bearing mice. The percentage of MDSCs and the numbers of CD8⁺ cells and gene expression of *IL-2*, *IL-10*, *IFN- γ* , and *TGF- β* in the control group were measured. The tumor sizes were measured in every group. Figure 4 shows empirical data.

(a)



(b)

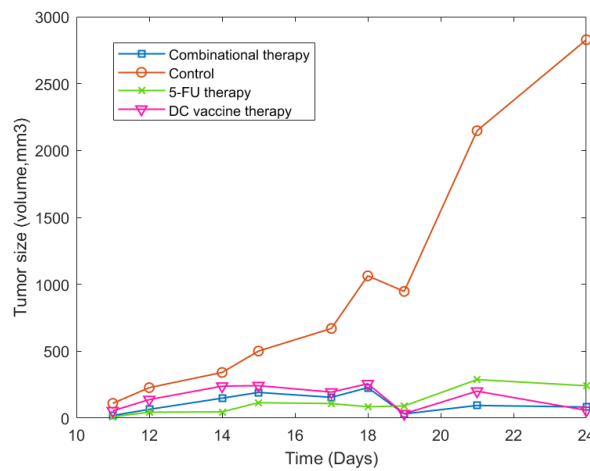


Figure 4. Delay of tumor growth in mice treated with dendritic cells (DC) and low-dose 5-Fluorouracil (5-FU). (a) schematic of the experimental design to evaluate the effects of low-dose 5-FU for myeloid-derived suppressor cells (MDSC) inhibition combined with DC vaccination in the B16F10 melanoma model. Melanoma bearing C57BL/6 mice were divided into 4 groups: the control (no treatment), the 5-FU group (5-FU injected with 3-days interval), the DC vaccine group (treated with 10^6 cells DC vaccine subcutaneously), and the combinational therapy group (treated with both DC vaccine and 5-FU). On days 13, 17, 19, 22, and 25 the tumor tissues and spleens were collected from animals in every group, and (b) tumor size was estimated by elliptical volume equation from diameters of the tumor.

Results of Agent-based Simulation Model Fitness to Control Group

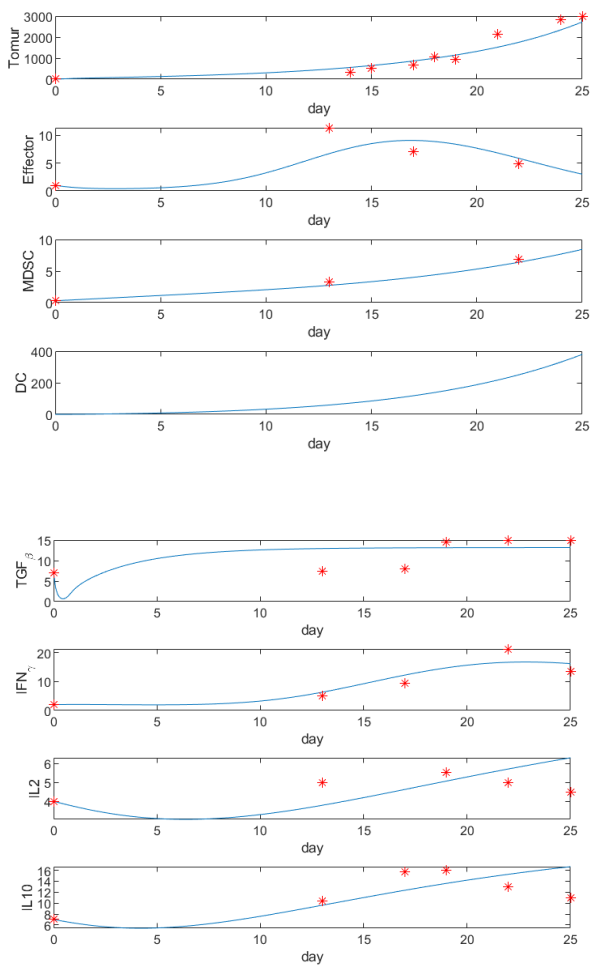
The proposed model was fitted to the data from the control group of empirical data. The coefficients of the models are listed in Table 1. Results of the model simulation and residual error of fitness to the tumor size data are presented in Figure 5.

Model Fitness to 5-FU Therapy Group

As mentioned earlier, parameters of the control

group are used to simulate the dynamics of the model output to the 5-FU therapy group data. Explained modifications of the equations were applied to the control group model to achieve the best fitness of model output to the data of the 5-FU therapy group. Results of the model simulation and residual error of fitness to the tumor size data of the 5-FU therapy group are presented in Figure 6.

(a)



(b)

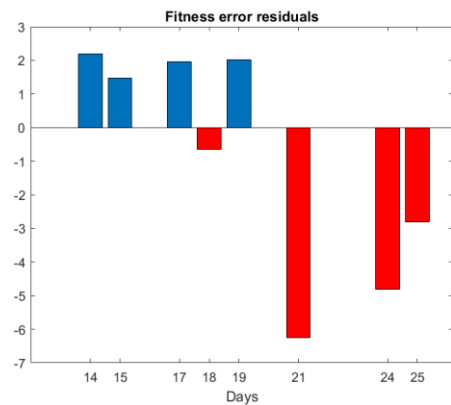
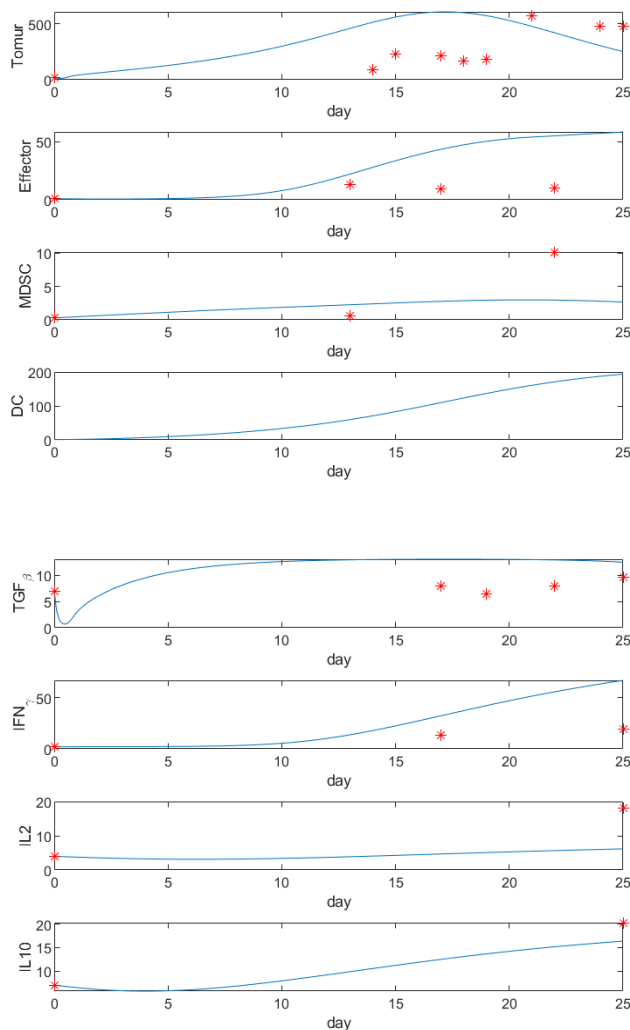


Figure 5. The agent-based model is fitted to the empirical data from the animal model. (a) Model output (blue line) and data points (red *) for the control group. The tumor size data in the first graph is the mean tumor size on days 14, 15, 17, 18, 19, 21, 24, and 25 for 14, 14, 11, 11, 8, 7, 4, and 1 mice, respectively. Graphs demonstrate good fitness between model output trends and empirical data for the control group. (b) Residual error of the model training step fitness to control group tumor size.

Low-dose 5-Fluorouracil and Dendritic Cell Vaccine Combination Therapy

(a)



(b)

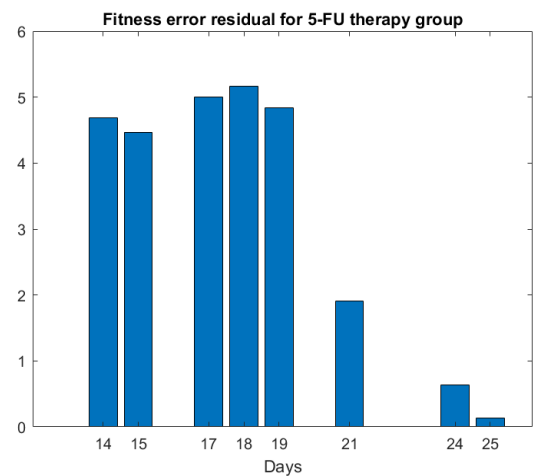


Figure 6. The agent-based model is modified to fit empirical data of the 5-Fluorouracil (5-FU) therapy group of the animal model. (a) Model output (blue line) and data points (red *) for the 5-FU group. The tumor size data in the first graph is the mean tumor size on days 14, 15, 17, 18, 19, 21, 24, and 25 for 14, 14, 11, 11, 8, 8, 5, and 1 mice, respectively. Graphs demonstrate good fitness between model output trends and empirical data for the 5-FU therapy group. (b) Residual error of the model training step fitness to 5-FU therapy group tumor size.

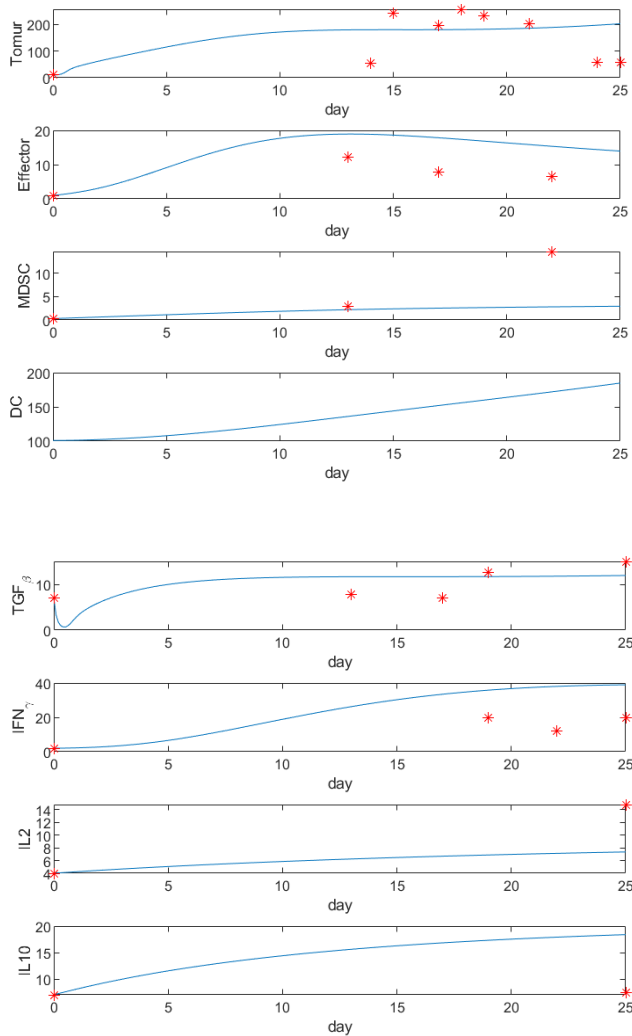
Model Fitness to DC Vaccine Therapy Group

The same procedure was done to simulate the dynamics of the model output to the DC vaccine group data. Explained modifications of the equations were applied to the control group model to achieve the best fitness of model output to the data of this group. Results of the model simulation and residual error of fitness to the tumor size data of the DC vaccine group are presented in Figure 7.

Model Fitness to the Combinational Therapy Group

Finally, the simulations of the 5-FU therapy and DC vaccine were combined by superimposition to demonstrate the dynamics of the model output to the combinational group data. The results show good adaptability of the model in combining these two therapy modes. Results of the model simulation and residual error of fitness to the tumor size data of combinational therapy group are presented in Figure 8.

(a)



(b)

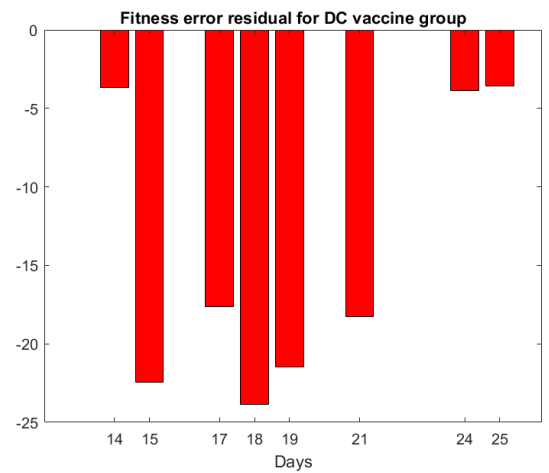
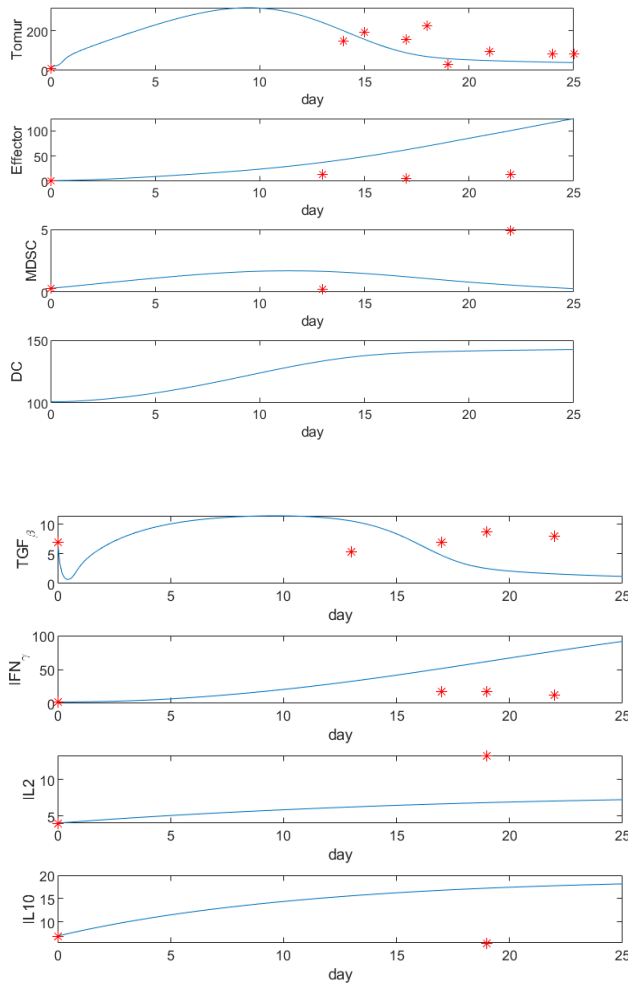


Figure 7. The agent-based model is modified to fit empirical data of the DC vaccine group of the animal model. (a) Model output (blue line) and data points (red *) for the 5-Fluorouracil (5-FU) group. The tumor size data in the first graph is the mean tumor size on days 14, 15, 17, 18, 19, 21, 24, and 25 for 12, 12, 9, 9, 6, 6, 4, and 1 mice, respectively. Graphs demonstrate good fitness between model output trends and empirical data for the DC vaccine group. (b) Residual error of the model training fitness to DC vaccine group tumor size.

Low-dose 5-Fluorouracil and Dendritic Cell Vaccine Combination Therapy

(a)



(b)

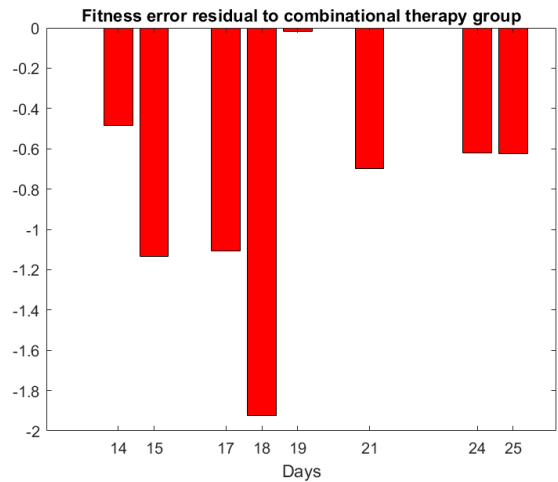


Figure 8. The agent-based model is modified to fit empirical data of the combinational therapy group of the animal model. (a) Model output (blue line) and data points (red *) for the 5-Fluorouracil (5-FU) group. The tumor size data in the first graph is the mean tumor size on days 14, 15, 17, 18, 19, 21, 24, and 25 for 14, 14, 10, 10, 8, 8, 6, and 2 mice, respectively. Graphs demonstrate good fitness between model output trends and empirical data for the combinational therapy group. (b) Residual error of the model training fitness to combinational therapy group tumor size.

DISCUSSION

Immunotherapy is a treatment based on immunosurveillance theory and has recently been used successfully to treat cancers. This method of cancer treatment attempts to improve the ability of an individual's immune response to reject the tumor immunologically rather than only removing tumor cells by surgery or radiotherapy.²² However, the efficacy of cancer immunotherapies is affected by the immunoregulatory tumor microenvironment comprising

of immunosuppressive cells such as MDSCs and Tregs. Therapies that target immunosuppressive mechanisms along with immunostimulatory methods are more effective tools in tumor regression.^{23,24} A combination of vaccines with chemotherapeutic agents and/or radiotherapy reported the successful control of cancer growth and/or achieve the synergistic effects.^{25,26} Namdar et al, introduced low noncytotoxic concentrations of 5-Fluorouracil (5-FU) as a safe adjuvant for DC-based cancer therapy.²⁷ Their work reports that not only low-doses of 5-FU have no adverse

effects on DC maturation and function but also improve the efficacy of DC-based cancer immunotherapy. Camargo et al presented that a Combination of DC vaccines with a low dose of 5-FU twice a week induced tumor regression in 77% of the CRC-bearing C57Bl/6 mice.²⁸ They have also reported that Combinational therapy reduced the number of circulating MDSC in comparison with untreated animals. The observed effects were attributed to the ability of low-dose 5-FU to increase the numbers of both CD4 and CD8 lymphocytes. Khosravanifar et al, have investigated DC immunotherapy with 5-FU as a combination strategy in a mouse melanoma model (F10-B16).²⁹ They have shown that the 5-FU and DC vaccine can empower the immune system to suppress tumor growth via reducing the number of MDSCs and increasing CTL cytotoxicity.

In the present study, the data that were collected in the animal experiment showed that receiving either low-dose 5-FU or DC vaccine can cause a decline in the tumor volume relative to the control group (Fig. 4). It is also noticeable from the MDSCs percentage compared among groups that the tumor growth rate reduction in groups that received 5-FU therapy is caused by the elimination of MDSCs from the microenvironment. However, the tumor growth rate in the DC vaccine group is mainly independent of MDSC percentage. Also, the empirical data shows that applying 9 doses of low-dose 5-FU from the first day of tumor inoculation with 3-days intervals or DC vaccine on the first day has no significant difference in tumor growth rate and both treatments protocols were successful in tumor regression with similar results. However, the dynamics of achieving these results are different. It may be suspected from the effector values in all groups that the 5-FU or DC vaccine did not change the maximum tumor-infiltrating lymphocytes in our results drastically. Since DC vaccine can improve the affinity of effector cells, this shortage of the effector number is compensated by increasing the killing power of individual effector cells in the model by combining the two therapy methods we have achieved to a better condition from the aspect of the immune system, both by reducing MDSCs as immunosuppressive agents as well as increasing the affinity of the effectors in the encounter with tumor cells. The dynamics of the tumor and immune system components specify the dominance of each component during tumor progression. Therefore, manipulation of the dominant components will help to get better results

in treatment. The roles of the immune system components during progression levels of the tumor, are not stable and changes over time. To capture these dynamics, it is necessary to study the immune system and tumor interactions by dynamic animal models rather than before-after assays. As applying dynamic animal models are more expensive because of an increasing number of animals required to achieve reliable results; using *in silico* models is more affordable. Therefore, combining cancer immunology knowledge with mathematical models in recent years has demonstrated beneficial effects on cancer therapy studies. Several mathematical methods have been used to model the relations of tumor and immune system to model an immunotherapy treatment. A delayed differential equation (DDE) set for modeling tumor growth and its interactions with the immune system by; using the empirical data was developed to propose an optimized immunotherapy treatment protocol with DC vaccine.³⁰ In this study, animal model results for the control group were used to adjust the model output to real data and several hypothetical treatments were simulated. There was no animal data to test the proposed treatment protocols. In another study, a mathematical model of DC therapy for melanoma (by using a compartmental model of the tumor microenvironment, blood, and spleen and the DC trafficking among these compartments) was proposed. The authors then presented the results of the hypothetical effect of modifying dose and injection times of DC vaccine without increasing the total dose of DC vaccine on tumor growth.³¹ Like the former study, there was no data presented in this paper to support the proposed treatment protocol. In another survey based on an ANN mathematical model, a new pattern for DC vaccination in fibrosarcoma murine models is presented.³² The ANN model was then used to achieve a treatment protocol for tumor regression and maximum prolongation of survival. Our recent work introduced an agent-based model based on interactions between tumor cells, effector cells, and the effect of MDSCs as an immunosuppressive agent.³³ To evaluate the effectiveness of MDSC reduction on the steady-state of the system, the impact of low-dose 5-FU injection was implemented to the model and several delivery protocols were simulated to determine the optimal delivery protocol hypothetically.

The present Agent-based model follows the behavior of the tumor and immune system properly. The model

Low-dose 5-Fluorouracil and Dendritic Cell Vaccine Combination Therapy

was developed so that it can be used on each group independently. The combination of therapy by 5-FU and DC vaccine are added together and the combinational therapy was modeled. This simplicity of the proposed model can help to understand the results of the combinational therapy and make the model a useful tool for studying different scenarios and assessing the combinational results. Testing mechanisms that contribute to immune response and determining the role of each component during tumor progression time promises to find new critical times to change the tumor and immune system balance in favor of the immune system. This idea is the main core of the study by Shafiekhani et al, to investigate the effect of perturbation of fuzzy ODE model parameters on dynamics of cells and the final state of tumor and immune system.³⁴

The structure of our agent-based model is valid for other tumor types and the relations and interactions are common among a collection of cancers. But the parameters of the model should be readjusted for other tumors' empirical data to be used in other studies. Also adding new immune system components and therapies are easily applied to the present model by adding new equations of their relations.

we can test mechanisms that contribute to immune response and determine the role of each component during tumor progression time. Using these more refined results, we will be able to suggest an optimal dosing and delivery protocol for single treatment therapy and combinational therapy. Simulations of these protocols will significantly speed up taking these new treatment protocols from bench to clinic.

CONFLICT OF INTEREST

The authors declare that they have no conflict of interest.

ACKNOWLEDGEMENTS

This study was supported by a grant (No. 28284) from the Tehran University of Medical sciences.

REFERENCES

1. Buessow SC, Paul RD, Lopez DM. Influence of Mammary Tumor Progression on Phenotype and Function of Spleen and In Situ Lymphocytes in Mice 2. *J Natl Cancer Inst.* 1984;73(1):249-55.
2. Seung LP, Rowley DA, Dubey P, Schreiber H. Synergy between T-cell immunity and inhibition of paracrine stimulation causes tumor rejection. *Proc Natl Acad Sci U S A.* 1995;92(14):6254-8.
3. Young MR, Newby M, Wepsic HT. Hematopoiesis and suppressor bone marrow cells in mice bearing large metastatic Lewis lung carcinoma tumors. *Cancer Res.* 1987;47(1):100-5.
4. Abedi-Valugerdi M, Zheng W, Benkessou F, Zhao Y, Hassan M. Differential effects of low-dose fludarabine or 5-fluorouracil on the tumor growth and myeloid derived immunosuppression status of tumor-bearing mice. *Int Immunopharmacol.* 2017;47(4):173-181.
5. Umansky V, Sevko A. Tumor microenvironment and myeloid-derived suppressor cells. *Cancer Microenviron.* 2013;6(2):169-77.
6. Umansky V, Sevko A, Gebhardt C, Utikal J. Myeloid-derived suppressor cells in malignant melanoma. *J Dtsch Dermatol Ges.* 2014;12(11):1021-7.
7. Shou D, Wen L, Song Z, Yin J, Sun Q, Gong W. Suppressive role of myeloid-derived suppressor cells (MDSCs) in the microenvironment of breast cancer and targeted immunotherapies. *Oncotarget.* 2016 Sep 27;7(39):64505-64511.
8. Namdar A, Mirzaei HR, Jadidi-Niaragh F, Ashourpour M, Ajami M, Hadjati J, Rezaei A. Multiple Low Doses of 5-Fluorouracil Diminishes Immunosuppression by Myeloid Derived Suppressor Cells in Murine Melanoma Model. *Iran J Immunol.* 2015;12(3):176-87.
9. Lala PK, Patt HM. Cytokinetic analysis of tumor growth. *Proc Natl Acad Sci U S A.* 1966;56(6):1735-42.
10. Spratt JS, Meyer JS, Spratt JA. Rates of growth of human neoplasms: Part II. *J Surg Oncol.* 1996 Jan;61(1):68-83.
11. Kuznetsov VA, Makalkin IA, Taylor MA, Perelson AS. Nonlinear dynamics of immunogenic tumors: parameter estimation and global bifurcation analysis. *Bull Math Biol.* 1994;56(2):295-321.
12. Kirschner D, Panetta JC. Modeling immunotherapy of the tumor-immune interaction. *J Math Biol.* 1998 Sep;37(3):235-52.
13. Arciero J, Jackson T, Kirschner D. A mathematical model of tumor-immune evasion and siRNA treatment. *Discrete and Continuous Dynamical Systems Series B.* 2004;4(1):39-58.
14. Byrne HM, Alarcon T, Owen MR, Webb SD, Maini PK. Modelling aspects of cancer dynamics: a review. *Philos Trans A Math Phys Eng Sci.* 2006;364(1843):1563-78.
15. Figueredo GP, Joshi TV, Osborne JM, Byrne HM, Owen MR. On-lattice agent-based simulation of populations of

- cells within the open-source Chaste framework. *Interface Focus*. 2013;3(2):20120081.
16. Figueredo GP, Siebers PO, Owen MR, Reys J, Aickelin U. Comparing stochastic differential equations and agent-based modelling and simulation for early-stage cancer. *PLoS One*. 2014;9(4):e95150.
 17. Allahverdy A, Rahbar S, Mirzaei HR, Ajami M, Namdar A, Habibi S, Hadjati J, Jafari AH. Extracting Mutual Interaction Rules Using Fuzzy Structured Agent-based Model of Tumor-Immune System Interactions. *J Biomed Phys Eng*. 2021;11(1):61-72.
 18. Inaba K, Inaba M, Naito M, Steinman RM. Dendritic cell progenitors phagocytose particulates, including bacillus Calmette-Guerin organisms, and sensitize mice to mycobacterial antigens in vivo. *J Exp Med*. 1993 Aug 1;178(2):479-88.
 19. de Camargo MR, Kaneno R, de Camargo MR, Vannini P, Kaneno R, Ostrand-Roseberg S. Low Dose Of 5-Fluorouracil Combined with A Dendritic Cell Vaccine Delays the Growth of Colorectal Cancer in Mice. *Biomed J Sci Tech Res*. 2020;29(4):22583-7.
 20. Vincent J, Mignot G, Chalmin F, Ladoire S, Bruchard M, Chevriaux A, Martin F, Apetoh L, Rébé C, Ghiringhelli F. 5-Fluorouracil selectively kills tumor-associated myeloid-derived suppressor cells resulting in enhanced T cell-dependent antitumor immunity. *Cancer Res*. 2010;70(8):3052-61.
 21. Lee TH, Cho YH, Lee MG. Larger numbers of immature dendritic cells augment an anti-tumor effect against established murine melanoma cells. *Biotechnol Lett*. 2007;29(3):351-7.
 22. Zhou J. Advances and prospects in cancer immunotherapy. *New J. Sci*. 2014;2014.
 23. Stewart TJ, Smyth MJ. Improving cancer immunotherapy by targeting tumor-induced immune suppression. *Cancer Metastasis Rev*. 2011;30(1):125-40.
 24. Whiteside TL. Disarming suppressor cells to improve immunotherapy. *Cancer Immunol Immunother*. 2012;61(2):283-288.
 25. Ménard C, Martin F, Apetoh L, Bouyer F, Ghiringhelli F. Cancer chemotherapy: not only a direct cytotoxic effect, but also an adjuvant for antitumor immunity. *Cancer Immunol Immunother*. 2008;57(11):1579-87. doi: 10
 26. Zitvogel L, Apetoh L, Ghiringhelli F, Kroemer G. Immunological aspects of cancer chemotherapy. *Nat Rev Immunol*. 2008;8(1):59-73.
 27. Namdar A, Mirzaei HR, Hafezi M, Khosravianfar N, Kheshtchin N, Mirzaei R, Hadjati J, Rezaei A. Low Noncytotoxic Concentrations of 5-Fluorouracil Have No Adverse Effects on Maturation and Function of Bone Marrow-Derived Dendritic Cells in vitro: A Potentially Safe Adjuvant for Dendritic Cell-Based Cancer Therapy. *Int Arch Allergy Immunol*. 2015;168(2):122-30.
 28. de Camargo MR, Kaneno R, de Camargo MR, Vannini P, Kaneno R, Ostrand-Roseberg S. Low Dose Of 5-Fluorouracil Combined with A Dendritic Cell Vaccine Delays the Growth of Colorectal Cancer in Mice. *Biomed J Sci Tech Res*. 2020;29(4):22583-7.
 29. Khosravianfar N, Hadjati J, Namdar A, Boghazian R, Hafezi M, Ashourpour M, Kheshtchin N, Banitalebi M, Mirzaei R, Razavi SA. Myeloid-derived Suppressor Cells Elimination by 5-Fluorouracil Increased Dendritic Cell-based Vaccine Function and Improved Immunity in Tumor Mice. *Iran J Allergy Asthma Immunol*. 2018;17(1):47-55.
 30. Qomlaqi M, Bahrami F, Ajami M, Hajati J. An extended mathematical model of tumor growth and its interaction with the immune system, to be used for developing an optimized immunotherapy treatment protocol. *Math Biosci*. 2017;292(15):1-9.
 31. Depillis L, Gallegos A, Radunskaya A. A model of dendritic cell therapy for melanoma. *Front Oncol*. 2013 Mar 19;3:56.
 32. Mirsanei Z, Habibi S, Kheshtchin N, Mirzaei R, Arab S, Zand B, Jadidi-Niaragh F, Safvati A, Sharif-Paghaleh E, Arabameri A, Asemani D, Hajati J. Optimized Dose of Dendritic Cell-based Vaccination in Experimental Model of Tumor Using Artificial Neural Network. *Iran J Allergy Asthma Immunol*. 2020;19(2):172-182.
 33. Allahverdy A, Moghaddam AK, Rahbar S, Shafiekhani S, Mirzaei HR, Amanpour S, Etemadi Y, Hadjati J, Jafari AH. An Agent-based Model for Investigating the Effect of Myeloid-Derived Suppressor Cells and its Depletion on Tumor Immune Surveillance. *J Med Signals Sens*. 20;9(1):15-23.
 34. Shafiekhani S, Jafari AH, Jafarzadeh L, Gheibi N. In Silico Assessment of 5-FU Therapy via A Mathematical Model with Fuzzy Uncertain Parameters. 2020, manuscript accepted for publication in *BMC Cancer*.